Taylor & Francis
Taylor & Francis Group

MINIMIZATION OF INDOOR TEMPERATURES AND TOTAL SOLAR INSOLATION BY OPTIMIZING THE BUILDING ORIENTATION IN HOT CLIMATE

Maamar HAMDANI[a, b], Sidi Mohammed El Amine BEKKOUCHE[a], Tayeb BENOUAZ[b], Rafik BELARBI[c], Mohamed Kamel CHERIER[a]

[a]*Unité de Recherche Appliquée en Energies Renouvelables, URAER, Centre de Développement des Energies Renouvelables, CDER, 47133, Ghardaïa, Algeria*
[b]*University of Tlemcen, BP. 119, Tlemcen R.p. 13000 Algeria*
[c]*Laboratoire Des Sciences De L'ingénieur Pour L'environnement Lasie, Universite De La Rochelle, France*

Abstract. In order to reduce the energy load, understanding the overall architectural design features and optimizing building orientation are important. They are guided by natural elements like sunlight and its intensity, direction of the wind, seasons of the year and temperature variations. The main aim of presented analysis is to give solutions for architects to design standard and low energy buildings in a proper way. The orientation effect of a non-air-conditioned building on its thermal performance has been analyzed in terms of direct solar gain and temperature index for hot-dry climates. This paper aims at introducing an improved methodology for the dynamic modeling of buildings by the thermal nodal method. The study is carried out using computer simulation. This study examines also the effect of geometric shapes on the total solar insolation received by a real building. As a result, the influence of orientation changing depends on the floors and exterior walls construction materials, the insulation levels and application of the inseparable rules of the bioclimatic design. Solar radiation is the most major contributor to heat gain in buildings.

Keywords: temperature, orientation, building materials, time lag, decrement factor, building size, geometric shapes.

Introduction

During certain synoptic conditions building orientation can have a great influence on the thermal behavior of different facades for two very different thermal regimes (for the very hot and very cold periods).

Design for orientation is a fundamental step to ensure that buildings work with the passage of the sun across the sky. Knowledge of sunpaths for any site is fundamental in design building facades to let in light and passive solar gain, as well as reducing glare and overheating to the building interior. Along with massing, orientation can be the most important step in providing a building with passive thermal and visual comfort. Orientation should be decided together with massing early in the design process, as neither can be truly optimized without the other.

Raychaudhuri *et al.* 1965, present the results of a year-round experimental investigation carried out to study the effect of orientation on the indoor thermal conditions of thirty-two occupied dwellings of similar plans and design specifications but having eight different orientations. From both the experimental observations and the theoretical computations, it is found that the dwellings facing south-east and south directions have better indoor climatic environment throughout the year. However, in 1985 (Anderson *et al.* 1985), the

Corresponding author:
M. Hamdani E-mail: *hamdanimaamar@yahoo.fr*

study was carried out for 25 climates in the United States. It was found that in all climates, when the more extensively glazed exposure is oriented to south, total loads are significantly lower than those in the same building oriented east or west. North orientation also produces lower total loads than east or west orientations in the southern two-thirds of the U.S., and roughly equivalent loads in the northern third. The impact of building location and climate and orientation on thermal comfort were investigated. Haase *et al.* 2009, prove that the orientation of a building depends on the climate.

Chwieduk, Bogdanska 2004 consider solar energy availability on different surfaces that constitute the envelope of a building. An analysis is presented to give recommendations for architects to help them design standard and low energy buildings in a proper way, including the integration of active and passive solar systems into building structure. For different periods of time, architects can decide on the orientation of the elements of a building envelope, including solar passive and active elements. To design the orientation and the inclination of building walls and roofs, to meet seasonally varying energy needs, the irradiation data for different azimuth and inclination angles for different period of time should be known (or calculated). The resulting modeled internal heat source rate of boundary elementary volume depends on the location of the volume, i.e. the orientation (azimuth) and the inclination (slope) angles of the outer surfaces have direct contact with the ambient surroundings. It is proved that distributions of daily energy demands for heating or cooling in months of the averaged year by every hour of the day for a room with the orientation and inclination under consideration are very similar to distributions of the daily solar irradiance of the surfaces of the same orientation and inclination at every hour of a day (Dorota 2008). According to Morrissey *et al.* (2011), the best solution to have a low cost, is to orient buildings in order to maximize their passive solar benefits. Design adaptability by change of orientation was modelled across two scenarios; current building energy efficiency standards and pending improved energy efficiency standards. The effect of size and overall energy efficiency rating was included in consideration of variance across orientations (Morrissey *et al.* 2011). In other studies, the authors have treated the case of a careful orientation of existing designs in order to optimize passive solar performance. This idea is the main

concern of this contribution, which also serves to test the case made elsewhere that passive design is a potentially significant contributor to thermal performance and, therefore, energy efficiency (Givoni 1991). Good orientation and location on site may potentially reduce the energy requirements of a typical dwelling by 20 percent (Spanos *et al.* 2005). Therefore, they ensured that there are two ways to ensure optimal orientation. The first is to analyse various parameters and ensure optimal design and orientation on a building by building basis, and the second is to develop "adaptable" designs which perform well across a range of orientations (Hoffman 1983; Balcomb *et al.* 1977). In addition, appropriate passive solar design should consider key building parameters such as building orientation, plan proportion and shape, facade glazing design and obstruction by surrounding buildings. Of these parameters appropriate orientation is the most fundamental and generally most easily addressed aspect of passive solar design. In addition, appropriate orientation can create potential for additional savings from more sophisticated passive solar techniques (Morrissey *et al.* 2011; Numan *et al.* 1999; Aksoy, Inalli 2006). By combining the optimization of shape and orientation, it is possible to obtain benefits that can lead to heat energy savings of 36% according It is generally agreed that a southern orientation is optimal for gaining heat in the winter and for controlling solar radiation in the summer. As a general rule, the longest wall sections should be oriented toward the south (Chwieduk, Bogdanska 2004). However, orientation can also be studied with a view to optimizing other parameters such as the total solar radiation received, building shape, ground plan surface, and the annual energy demand in article of Aksoy, Inalli (2006). However, it is generally agreed that a southern orientation is optimal for gaining heat in the winter and for controlling solar radiation in the summer, and the longest wall sections should be oriented toward the south. Orientation can also be studied with a view to optimizing other parameters such as the total solar radiation received, building shape, ground plan surface, and the annual energy demand (Mingfang 2002; Pacheco *et al.* 2012). Indeed, Ozel *et al.* (2007) found that for various wall orientations in both summer and winter conditions, the optimum location of insulation was obtained from consideration of time lag and decrement factor. In other research (Keplinger 1978), there is proved that the cost of systems and solar devices may be considered high, it is insignificant

compared to the irretrievable cost of improper orientation or design. Once a building is poorly located or faultily oriented, the opportunity for correction is gone forever, or the cost is prohibitive. A building properly designed and oriented can greatly reduce the demands on the heating and cooling system, in turn reducing the needed area of expensive solar collectors. Reducing the initial costs of solar systems will speed acceptance and implementation of solar energy utilization. While Givoni (1994), discusses objectives and principles for building design, from the human comfort aspects, in regions with hot humid summers and mild winters. The issues discussed are: building layout, openings and ventilation, thermal mass, orientation with respect to the sun and the wind.

The improvement of building thermal behaviour is a very important challenge because of the electrical consumption, thermal discomfort generates undesired temperatures either for the summer season or even the winter season, both situations result a need for heating and cooling within the building which urges to use automatically the electric power. The use of building thermal simulation software is necessary to achieve this task. But, before using such a program, one must ensure that its results are reliable. To do so, a methodology must be applied including the verification of numerical implementation and experimental validation.

1. Objective of the study

This paper provides a simplified analysis method to predict the impact of the orientation for a building on its instantaneous temperature. A proposed model is developed based on detailed simulation analyses utilizing several combinations of building geometry, orientation, thermal insulation level, glazing type, glazing area and climate. The aim of this paper is to determine the optimum orientation due to this type of climate to control the maximum indoor temperatures and direct solar gain. The originality of this paper lies in determining the favorable orientation taking into account the building compactness, the location of the zone, the geometrical shape, the building size and building materials

2. Nodal analysis applied to heat conduction and coupling with superficial exchanges

The computing of temperatures, whether for air or for layers of walls, and also the perception of dynamic aspect of thermal transfer are of paramount impor-

tance. A review of the literature reveals many applied methods of such modeling approaches for residential buildings. Polish standards (PN-B-03406: 1994; PN-EN 12831: 2006) on calculation methods of heat demand for space heating of buildings take into account averaged global monthly solar radiation incident on surfaces with inclination with different inclination and azimuth angle (Chwieduk, Bogdanska 2004). Energy flow can be modeled using a thermal resistance method corresponding to calculation of equivalent electrical circuit flow (Gordon 2001). However, to describe the energy flow using the thermal resistance method, it can be assumed that heat transfer between temperature nodes is proportional to respective temperature difference (Dorota 2008). It should be stated that the main aim of this paper is to present some aspects of modeling the energy balance of a room in regard to the impact of solar energy. Raychaudhuri *et al.* (1965) provide matrix method of computation used for predicting the indoor temperatures. This method, although it has its limitations, is certainly capable of presenting comparative performance on variously oriented dwellings. But it would be rather impossible to take into account precisely the occupied-in conditions and other uncertain variables in the computation for occupied dwellings.

In this contribution, thermal nodal method was used to apprehend thermal behavior of air subjected to varied solicitations. The nodal analysis is a powerful method of investigation in thermal systems. It has been used in several branches such as solar energy systems (Saulnier, Alexandre 1985), micro-electronics (Auger *et al.* 1981) or also the spatial field (Chapman 1984). We will gradually use this approach in the domain of building's physics and we'll interest ourselves in the automatic generation of nodal models.

A simplified approach allows representing the multilayer system by a model based on an electrical analogy proposed by Rumianowski *et al.* (1989), and then it was taken by Cron *et al.* (2003). It is often used when we intresse to the determination of the temperature of any node inside a wall. The following Figure 1 is an illustration of the decomposition principle.

The equivalent resistances are calculated by the following formulas:

$$n = n_A + n_B; \quad R_A = \sum_{k=1}^{n_A} \frac{e_k}{\lambda_k S_k}; \quad R_B = \sum_{k=n_A+1}^{n} \frac{e_k}{\lambda_k S_k}. \quad (1)$$

Heat capacities are determined as follows:

$$C_A = \sum_{k=1}^{n_A} \rho_i Cp_i e_i S(1-\beta_i); \quad C_B = \sum_{j=n_A+1}^{n} \rho_j Cp_j e_j S_j \delta_j; \quad (2)$$
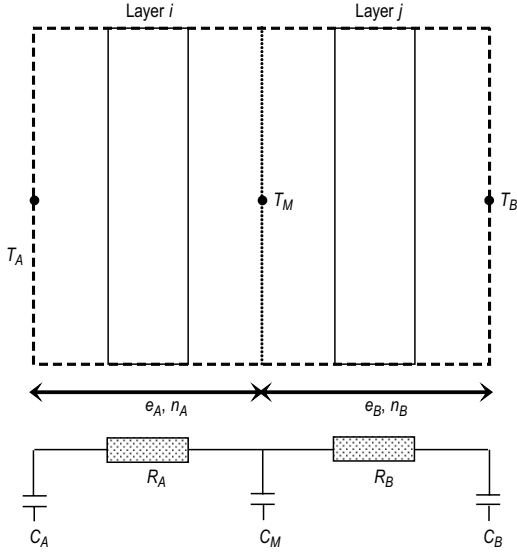
Fig. 1. Wall spatial discretisation and conduction model

$$C_M = \sum_{k=1}^{n_A} \rho_i \, Cp_i \, e_i \, S_i \beta_i + \sum_{j=n_A+1}^{n} \rho_j \, Cp_j \, e_j \, S_j \left(1-\delta_j\right); \quad (3)$$

$$\beta_i = \frac{\dfrac{e_i}{2\,\lambda_i\,S_i} + \displaystyle\sum_{k=1}^{i-1} \dfrac{e_k}{\lambda_k\,S_k}}{R_A}; \quad \delta_j = \frac{\dfrac{e_j}{2\,\lambda_j\,S_j} + \displaystyle\sum_{k=n_A+1}^{j-1} \dfrac{e_k}{\lambda_k\,S_k}}{R_B}. \quad (4)$$

The energy balance of the building for surfaces is represented by equations 5–7:

$$C_A \frac{dT_A}{dt} = \frac{T_M - T_A}{R_A} + \sum S\, F_{Surf-i}\, \sigma \left(T_i^4 - T_A^4\right) +$$

$$S\, h_{conv}\left(T_{air} - T_A\right); \quad (5)$$

$$C_B \frac{dT_B}{dt} = \alpha\, S\, G + \frac{T_M - T_B}{R_B} +$$

$$\varepsilon\, S\, \frac{1-\cos\beta}{2} \left(T_{Ground\ outside}^4 - T_B^4\right) +$$

$$\varepsilon\, S\, \frac{1+\cos\beta}{2} \left(T_{Sky}^4 - T_B^4\right) + S\, h_{conv\,amb}\left(T_{amb} - T_B\right); \quad (6)$$

$$C_M \frac{dT_M}{dt} = -\frac{T_M - T_A}{R_A} - \frac{T_M - T_B}{R_B}; \quad (7)$$

$$h_{conv\,amb} = 2.8 + 3.3\, V_{Wind}; \quad (8)$$

$$T_{Sky} = 0.0552\, T_{amb}^{1.5}, \quad (9)$$

where e – thickness (m); n – number of node; α – absorption coefficient; ε – thermal emissivity; G – the incident global irradiation on the surfaces (W m^{-2}); S – surface (m^2); λ – thermal conductivity (W K^{-1} m^{-1}); C_p – specific heat (J kg^{-1} K^{-1}); ρ – density (kg m^{-3}); F – form factor between the exchange surfaces; σ – Stephane-Boltzmann constant (W m^{-2} K^{-4}); V_{Wind} – wind speed (m s^{-1}); $h_{conv\,amb}$ – coefficient of heat flux exchanged by convection (W).

In the multizone-zone model a given building is made up with a certain number of rooms, walls, doors and also glass windows. The physical model of the building is obtained by assembling thermal models of each element. The different zones' temperatures (principal variables) are linked together through heat conduction and air movement.

We developed in Refs (Bekkouche *et al.* 2009, 2011, 2013a, 2013b) mathematical models based on first law of thermodynamics were elaborated to obtain different air temperatures of the inside parts. But in this paper, we make a coupling between the equations proposed by Rumianowski *et al.* (Mora 2003) and equations of a building thermal energy model found in the TRNSYS user manual (TRNSYS16 2004; Schmidt 2004; Sakulpipatsin *et al.* 2010). The building energy balance for a zone is a balance model with one air node per zone, representing the thermal capacity of the zone air volume. The building power balance for a zone is shown as equation 10 representing the variation of the power energy of the air in the zone in the time interval dt:

$$\rho_{air}\, C_{air}\, V_{air}\, \frac{dT_{air}}{dt} = Q_{Gain} + Q_{Surf} +$$

$$Q_{heating} + Q_{cooling} + Q_{Inf} + Q_{Vent}. \quad (10)$$

With thermal powers are algebraic values: T – temperature (K); ρ_{air} – air density (kg m^{-3}); C_{air} – the specific heat of air, it is assumed constant and estimated at 1008 (m^2 s^{-2} K^{-1}, J kg^{-1} K^{-1}); V_{air} – air volume (m^3); $Q_{heating}$ – thermal power provided by heating equipment (W); $Q_{cooling}$ – thermal power provided by cooling equipment (W); Q_{Inf} – thermal power gain due to air infiltration (W); Q_{Vent} – thermal power gain due to air ventilation (W); Q_{Surf} – thermal power due to exchange between the air and, (i) walls inner surfaces and (ii) windows and doors, (W); Q_{Gain} – direct solar gain due to openings (W).

The boundary conditions of the system include the nodes of the inner surface for all surfaces of the zone, including radiative energy flows. We also note that the energy of an active layer and the energy stored in the walls are not part of this energy balance, but they are part of detailed balance for surfaces.

The transfer rates of thermal energy of infiltration and ventilation air flow are respectively calculated by equations 11 and 12.

$$\dot{Q}_{Inf} = \dot{m}_{Inf}\, C_{air}\left(T_{air} - T_{out}\right); \quad (11)$$

$$\dot{Q}_{Vent} = \dot{m}_{Vent}\, C_p\left(T_{Vent,out} - T_{Vent,int}\right), \quad (12)$$

where $\dot{m}_{Inf}$ – the air flow due to infiltration (kg/s); $\dot{m}_{Vent}$ – the air flow due to ventilation (kg/s); T_{int} – ir temperature inside the building (K); T_{out} – air temperature outside the building (K); $T_{Vent,out}$ – air temperature at the ventilation outlet (K); $T_{Vent,int}$ – air temperature at the inlet ventilation (K).

Thermal energy due to exchange between the air and walls inner surfaces are calculated by equation 13:

$$Q_{Surf} = \sum S h_{Conv} \left(T_{Surf} - T_{air} \right), \qquad (13)$$

where T_{Surf} – air temperature walls inner surfaces (K); h_{Con} – the convective transfer coefficient (W m^{-2} K^{-1}). Numerical formulas are given in Table 1.

3. The nodal structure and description of the building

A given building is composed of a certain number of rooms, walls, doors and also glass-windows. At the beginning of this variable description, the building's decomposition into a certain number of zones is a simulation parameter. Therefore, the splitting up of the building into thermal zones induces the setting of nodes of temperature by zone. A certain number of information fields are connected to a node, traducing for instance the allocation of a node to a zone or also the topology of the global electrical network associated with the building. Considering the objective to be reached, we have been induced to assign a type to each node. Indeed, relative to the equations, the nodes are concerned with different phenomena. For instance, a wall node is going to concern terms of heat conduction. This same node, depending on its location, can also concern convective process. On the external face of the envelope's wall, the surface node is concerned with outdoor radiative and convective exchanges. We have to note that the size of this structure can quickly become significant, a building having most of the

time several zones and for each zone several walls and glass-windows. This structure's size being linked to the dimensions of the systems to be solved, the notion of calculation time must not be overlooked.

The study was carried out on a building in Ghardaïa. The exterior envelope, apart from contributing to the energy savings during the entire life span of the building by controlling the energy exchange between indoor space and environment, also promotes the development of a comfortable indoor environment. Figure 2 is a schematic outline of apartment building, the house has a habitable area of 71.3 m², and wall heights are equal to 2.8 m while the other dimensions are shown in detail in Figure 2. The flooring is placed on plan ground to lodge the ground floor. The concrete of the flooring is directly poured on the ground thus minimizing losses. Floor tiles are inter-

Fig. 2. Descriptive plane: southern orientation

Table 1. Expression of convective transfer coefficients (George 1999)

Surface description	Flow regime	Condition	Expression
Vertical wall	Laminar regime	$10^4 <$ Gr Pr $< 10^9$	$h_{Conv} = 1.42 \, (\Delta T/L)^{1/4}$
	Turbulent regime	Gr Pr $> 10^9$	$h_{Conv} = 1.31 \, (\Delta T/L)^{1/3}$
An upper surface of an hot horizontal plate or an underside surface of a cold plate	Laminar regime	$10^4 <$ Gr Pr $< 10^9$	$h_{Conv} = 1.32 \, (\Delta T/L)^{1/4}$
	Turbulent regime	Gr Pr $> 10^9$	$h_{Conv} = 1.52 \, (\Delta T/L)^{1/3}$
An underside surface of a hot plate or an upper surface of an cold plate	Laminar regime	$10^4 <$ Gr Pr $< 10^9$	$h_{Conv} = 0.59 \, (\Delta T/L)^{1/4}$
	Turbulent regime	Gr Pr $> 10^9$	

Note: Gr – Grashof number; Pr – Prandtl number; L length of the plate (m); ΔT – temperature difference between the surfaces and volumes exchange (K).

imposed, it is an end coating resisting to corrosion and chemical agents. The roof is composed of cement slabs and concrete slab made so that it handles the load and be economical. A roof sloping of 5° allowed water evacuation through several openings. Until now the flat roofs are considered as nest infiltration and as architectural solution. Windows and doors contribute significantly to the energetic balance. Their contribution however depends on several parameters as: local climate, orientation, frame, relative surface (window-flooring), and concealment performance during night and sunny days. In this case focus is made particularly on windows and doors dimensions and all are made of woods. The apartment has a surface of 95.74 m² with an occupied space of 71.3 m².

A certain number of information fields are connected to a node, traducing for instance the allocation of a node to a zone or also the topology of the global electrical network associated with the building. We have been induced to assign a type to each node. Indeed, relative to the equations, the nodes are concerned with different phenomena. Then, it appears necessary to attribute a type to each node. Table 2 gives the types of nodes encountered. For a given building, when the node structure is established, it is easy to fill up each element of the mathematical model. Indeed, we have just to sweep the node structure and attribute the relevant terms. Then, the structure will include six zones' numbers (Figure 3).

Table 2. Types of nodes encountered

Node	Type
●	Outdoor surface node of outside wall
●	Internal node of outside wall
◉	Indoor surface node of outside wall
●	Outdoor surface node of window
●	Internal node of window
◉	Indoor surface node of window
◉	Indoor surface node of inside and outside door Outdoor surface node of inside door Outdoor surface node of outside door
●	Internal node of inside and outside door
●	Outdoor surface node of outside door
●	Dry indoor air temperature
●	Outdoor and indoor surface node of inside wall
◉	Internal node of inside wall
●	Surface node of ground
●	Internal node of ground
◉	Terminal node of ground
◉	Outdoor surface node of outside roof
◉	Internal node of outside roof
◉	Indoor surface node of outside roof

In Ghardaïa region building envelops or outer wall consisting of a heavy structure generally constituted of stones (40 cm thick), jointed and surrounded by two layers having thickness of 1.5 cm of mortar cement. The most inner face is coated with 1 cm thick plaster layer. The inner walls (or splitting walls) whose sides are in contact only with the internal ambient are
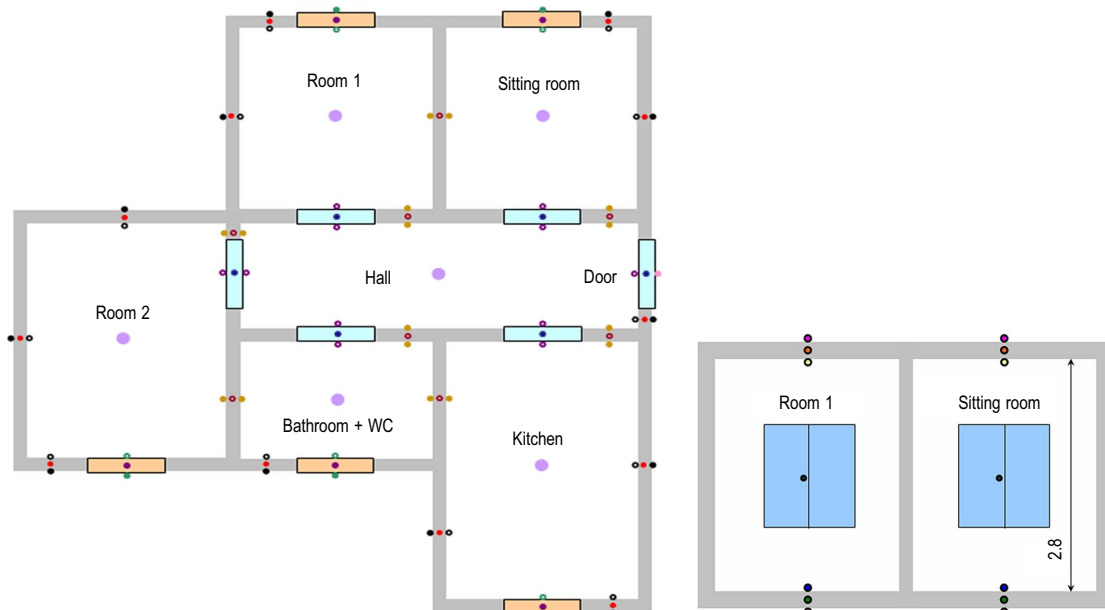

Fig. 3. Descriptive plane: southern orientation

considered to be of heavy structure constructed of stones of 15 cm width jointed and surrounded by two mortar cement layer of 1.5 cm thick and two layers of 1 cm thick of plaster (Table 3).

Windows and doors contribute significantly to the energetic balance. Their contribution however depends on several parameters as: local climate, orientation, frame, relative surface (window-flooring), and concealment performance during night and sunny days. In this case focus is made particularly on windows and doors dimensions and all are made of woods. Windows and doors have significant impacts on a building's energy usage, as they contribute to a building's heating and cooling loads as well as lighting if daylighting sensors and controls are deployed. Windows shall be designed to limit air leakage. The air infiltration rate shall not exceed 2.8 m³/hr per linear meter of sash crack when tested under a pressure differential of 75 Pa (George 1999). The used characteristics are given in Table 4.

If we consider that the habitat is poorly insulated, we use the U-value in the first case for glazing, and if the thermal insulation is reinforced, we use the values of the second case. For our study, we consider that the window composition comprises in addition

Table 4. Thermal properties, thicknesses of walls and building envelope characteristics

Glass Type		U-Value
Flat Glass Case 1: without thermal insulation	Single pane, clear For all windows	5.91
Insulating Glass Case 2: with thermal insulation	Double pane, clear, 12.5 mm air space For WC and bathroom	3.18
	Double pane, with low emittance coating e = 0.20 For rooms 1 and 2, kitchen and sitting room	2.21

to the configuration given in table 4, wood blinds usually separated from the previous configuration by an air gap of 2 cm. We assume that the heat transfers through windows are only by conduction. However, the doors are made of wood with a thickness of 2 cm: $\lambda = 0.14$ Wm^{-1}K^{-1}, $\rho = 500$ kg m^{-3} and Cp = 2500 J kg^{-1} K^{-1}, λ, ρ and Cp are respectively thermal conductivity, density and specific heat). Each wall type is described in Table 3. Some thermal properties of the materials are the usual values found in reference (Bekkouche *et al.* 2013a, 2013b; Silvana *et al.* 2009; Mazioud *et al.* 2010; Howlader *et al.* 2012).

Table 3. Thermal properties, thicknesses of walls and building envelope characteristics

		Material and wall composition	L, m	λ, W m^{-1} K^{-1}	ρ, kg m^{-3}	Cp, J kg^{-1} K^{-1}
Exterior walls	Type-1 wall	Mortar cement	0.015	1.4	1800	1000
		Stone	0.4	2.3	2000	1000
		Mortar cement	0.015	1.4	1800	1000
		Plaster	0.01	0.56	1400	1000
	Type-2 wall	Plaster	0.015	0.56	1400	1000
		Brick	0.3	0.81	1800	835
		Plaster clay	0.005	0.45	1200	840
Interior walls	Type-1 wall	Mortar cement	0.015	1.4	1800	1000
		Plaster clay	0.01	0.45	1200	840
		Stone	0.15	2.3	2000	1000
		Plaster clay	0.01	0.45	1200	840
		Mortar cement	0.015	1.4	1800	1000
	Type-2 wall	Plaster clay	0.01	0.45	1200	840
		Brick	0.2	0.81	1800	835
		Plaster clay	0.01	0.45	1200	840
Ground		Tiling	0.025	6.14	2300	875
		Cement	0.02	1.4	1800	1000
		Concrete dense	0.2	2.4	2400	800
Roof		Plaster	0.015	0.56	1400	1000
		Lightweight concrete	0.12	0.33	800	719
		Mortar cement	0.015	1.4	1800	1000

4. Experimental validation

This model took into account only thermal exchanges thus air stratification, whereas wind influence on air infiltration and water diffusion into walls body were not considered. Also states changes are not considered therefore storage of latent heat and moisture effects were neglected. The moisture problem does not arise in this building and in addition the climate is dry and the used building materials are generally ecological materials. Implementing the general law of building energy conservation, we arrive to a non stand alone system governed by one hundred and forty one non linear ordinary differential equations. Subsequently, it is essential to implement numerical methods that compute these temperatures. Designed to solve such problems, Runge-Kutta fourth order numerical method was used to apprehend thermal behavior of walls and air subjected to varied solicitations. The elaborated interactive programs allowed a better understanding heat transfer phenomenon of walls and air under dynamic regime. Windows and black-out curtains remained closed all over the period. The instantaneous temperatures of air and wall surfaces were calculated by entering the measured meteorological data.

The steps of this scientific method are: test of the hypothesis by doing an experiment, data analyses, communicate the results and draw a conclusion. The scientific method, used for most experiments, has several steps that we will need to follow carefully in order to make sure that the experiment is accurate and accepted as possible. The experimental method is usually taken to be the most scientific of all methods. In order to accomplish the measurement phase, a data acquisition unit of type Fluke Hydra Series II which in spite of its high accuracy, it accumulates some errors, not really considerable. Data acquisition systems are used extensively in many fields in order to accurately acquire and log data for measurement and analysis. Technicians know that they can count on Fluke to deliver quality measurements which meet all of their acquisition and analysis needs. Fluke data acquisition systems are perfect for small to medium scale process monitoring and testing, plugs into existing network allowing to quickly and easily sending data directly to PC. Hydra Fluke for Windows is a configuration and data management program. This program is available as a 32-bit application, contains modem support for remote data communications, and is available with or without Trend Link for Fluke trending and data analysis capabilities. Trend Link is a comprehensive trend plotting and analysis package that plots data graphically in real time. Calibrated type-K thermocouples were used to measure temperatures, their measuring principle is based on Seebeck effect. It produces a voltage when the temperature of one of the spots differs from the reference temperature at other parts of the circuit. For recording the temperatures of south and north walls, five thermocouples were placed in different locations of walls. Also, the temperatures of the internal ambient air were registered by placing other five thermocouples in different points. The plotted temperatures experimental values are those corresponding to the average of the registered ones. We introduced the thermocouples so that:

First is located in the center of the sitting room.

The second and the third are placed on the middle axis of the horizontal plane at 1.4 m in height so that each thermocouple is at 20 cm of the southern wall and the Northern wall.

The others thermocouples were inserted into the normal line which passes through the first thermocouple, they were implanted in such way the distance between the thermocouples and the walls (the roof and floor) will be about 10 cm.

Indeed, we judged that five thermocouples are largely sufficient because the temperature gradients are not really significant. According to the measurements in summer and for any position of the vertical plane, the maximum difference between air temperature at a point near the roof and another point on the same normal and at proximity to the ground does not exceed the value of 0.85 °C. Similarly, for any height, the maximum variation in temperature is about 1 °C between two points, one near the southern wall and the other near the northern wall, which lie along the same axis and same horizontal plane.

Then to measure the temperatures of the walls, we introduced the five thermocouples on surfaces of the walls by respecting the same distances. The first will be at the center, the second and the third will be on the vertical line which passes by the center and the last thermocouples will be on the horizontal line which passes by the center. The data were collected at 30 minutes intervals.

One of the main problems with most buildings in Ghardaïa, is that the envelope is not designed to cope with the extreme summer climate. The hot summer

outside air penetrates into the building and increases the cooling load. The external walls also readily conduct solar gains to the inner wall surface, which then warm and radiate into the room.

For the purpose of proper design of a modern low energy building it is necessary to calculate solar radiation on surfaces with different inclinations and orientation. The sets of averaged hourly sums of solar radiation, global and difusse, are applied as input data for simulation of solar radiation availability for various surfaces. To estimate the incident global irradiation, we have selected Perrin Brichambaut model that utilizes the atmospheric Linke turbidity factor in order to compute direct and diffuse components of solar irradiation. Absorption and diffusion caused by atmospherical particles are expressed in terms of the Linke turbidity factors. From these factors direct and diffuse irradiation are determined in case of clear sky model (Capderou 1987; Mefti *et al.* 1999; Kasten *et al.* 1980, 1989, 1996). We are interested in determining the incident irradiation on the roof (horizontal) and the vertical surface of external walls. Solar radiation distributions on the exterior façades of the zone, as in 20 min time steps for January and July are shown in Figure 4 under clear sky condition.

As seen, south façades receive the greatest total annual irradiation; they do not receive the maximum in summer, because the sun is too high in the sky. During winter the sun is at a much lower altitude and it is then they receive the maximum radiation. The two peaks in the morning and evening at respectively eastern and western walls are due to the influence of direct gain during these hours; the dome in between represents exclusively the diffuse radiation that occurs

at these times. At the east, high direct gain occurs in the morning hours and only diffuses radiation in the afternoon. The direct solar beam drops down at solar noon. At the south, diffuse and direct radiations coexist with a peak at solar noon.

This summer period was characterized by sunny days with high solar irradiance. The outdoor air temperature oscillated between 30.55 °C and 46.75 °C, with a mean value around 37.98 °C. The results, i.e., the simulation and the experimental temperatures for the air temperature profile are presented in Figure 5 for the type-1 walls.

The sitting room air temperature reaches its calculated maximum value of 37.54 °C and its measured maximum value of 37.74 °C around 23:00, and reaches its calculated minimum value of 36.1 °C and its measured minimum value of 35.58 °C around 11:00. The mean thermal amplitude was 3 °C on the temperature for calculated values and 2.79 °C on the temperature for measured values.
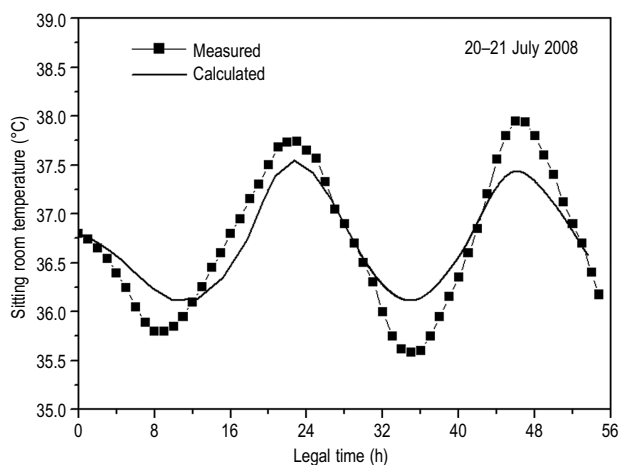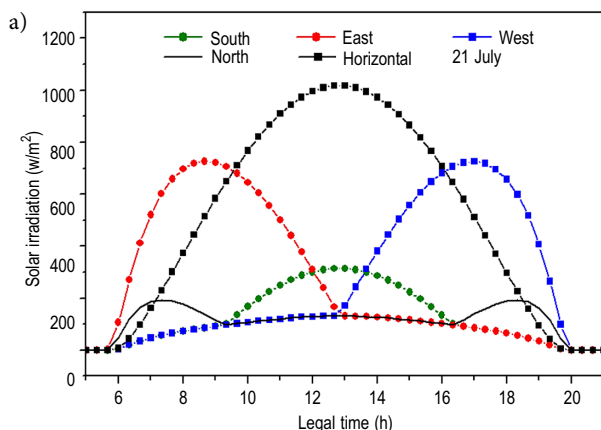

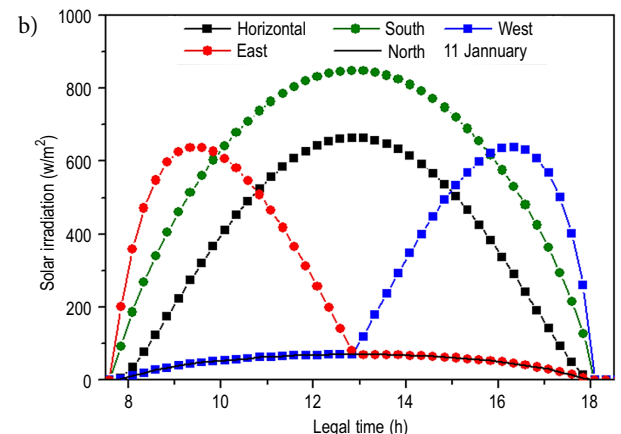Fig. 5. Measured and simulated temperature of sitting room

Fig. 4. Solar radiation at the exterior zone façades: the 21 of July (a) and 21 of January (b)

Indeed, this new numerical model for this building was also applied to the days of the winter season. Figure 6 shows the measured temperatures and those predicted by the identified model; represents temperatures curves of the internal air. All time traces shown are for the 54 hour time period mentioned above, the inputs used for these simulations are obtained from measured data during midnight of January 10, 2009 to 06:00 of January 13, 2009, which is part of the validation data set. The calculation result is compared with the measurement result. These days correspond to a clear sky and an ambient temperature between 6 °C and 14.5 °C, wind speed varies randomly between 3 m/s and 5 m/s in time. Running the program for several solicitations allows us to obtain this figure.

The found results show that the measured temperatures of the sitting room were found to be between 17.7 °C and 19.3 °C and between 17.55 °C and 19.2 °C for the simulated temperatures. The comparison proves as a whole acceptable, with a mean difference which not exceeds the order of 0.8 °C for air temperature. The margin of error is greater in this period compared to the summer. This margin is justified by the weather which is not stable: wind speed varies greatly in very complex. The input data, ie, ambient temperature and wind speed were included in the program by determining an interpolation function (polishing polynomial) that identifies each parameter to ensure the execution speed of the program designed. In this situation, randomized evaluation of these parameters does not establish the exact functions that properly approaching the experimental values.

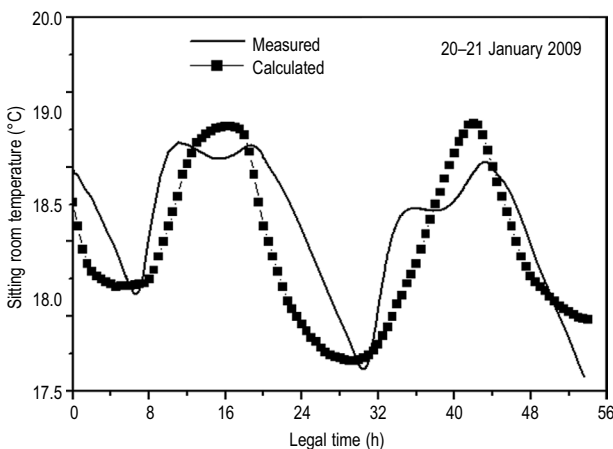The prediction of air temperatures from this model of a whole building is a step forward in the simulation process that helps the comprehension of the building behavior, the improvement of the building envelope, and the estimation of the comfort levels inside it. This simplified method is good approach to the understanding of the thermal behavior of air in a real building.

5. Result and discussions: ideal orientation

Along with massing, orientation can be the most important step in providing a building with passive thermal and visual comfort, generally used to refer to solar orientation which is the sitting of building with respect to solar access. Although any building will have different orientations for its different sides, the orientation can refer to a particular room, or to the most important facade of the building. In these studies, the orientation of the building as well as the relative dimensions of surfaces facing different directions would have to be considered. These studies are very useful for good planning to ensure design which agrees with a low-energy building.

5.1. Indoor temperature
5.1.1. According to the area's location

Figure 7 gives an overview of the sitting room temperatures during the days of July 24–25. These two days are characterized by a totally clear sky, an intensive solar radiation, an outdoor ambient temperature between 32 °C and 47 °C in the shade and a very low wind speed. In summary, the climatic conditions correspond to extremely hot days. From these results, we note that the obtained temperatures are very high. The higher interior air temperature during the evening hours is caused by the thermal storage. Thermal storage or thermal inertia of any wall can be defined as the maximum minus minimum surface temperature (temperature variation interval). The difference between the peaks of air temperature does not exceed the threshold of 1.7 °C; this can be justified by the high thermal inertia that promotes stable indoor temperatures because the difference between the peaks of external air temperature can reach around 15 °C.

It is known that, in the East and West facades, the low position of the sun can not glare treatment. The results predict that the west orientation is the least favorable. In the afternoon, the room is very glare and overheated, the sun leads to the overheating due to the long exposure time (07 hours: see Figure 4). In addition to that, the largest amount of daily radiation in-

Fig. 6. Measured and simulated temperature of sitting room

cident on the West side will be received during this period. It has approximately 92.56% of the total daily radiation which is estimated at 4025 Wh/m². In addition to this, the thermal phase shift caused by the high thermal inertia is another indicator that reflects the number of hours required (it is estimated at 06:03, show Figure 7) for the heat transfer through the wall. Moreover, the South and East orientations are more favorable before 21:00 with a slight advantage for South orientation in the morning and a net advantage to the East direction in the evening. Regarding the north direction, it may become more favorable between 24:00 and 07:30. Knowing that the maximum value of the room temperature is reached at 14:42, we found that the thermal phase shifts of the South, North, East and West directions are estimated at 07:49, 06:07, 07:51 et 06:03 respectively. It can be drawn from these indications that the thermal phase shift depends on the building's orientation.

Some variables with that are related to building shape and which influence heating and cooling requirements are the following: compactness index; the height of walls, climate; and the characteristics of the building envelope. These characteristics are crucial variables that should be taken into account because they are relevant to the energy requirements for maintaining the building at a comfortable temperature. The proper use of compactness index parameters will noticeably improve the internal temperature of the building. The compactness of a building, indicated by the S/V ratio (S: area of building envelope surface, V: volume of the building) has a considerable influence on the heating energy demand of buildings. The compactness is better when the compactness index is lower.

In this example, it is assumed that the building is a house with two fronts; the South and the North side if we refer to Figure 2. That is to say, we assume that the building is in a rural region. This means that the compactness index will decrease from 0.5882 (the case of the first example) to 0.27.

According to Figure 8, the most favorable orientations are those of the South and North with a small advantage for the North orientation. These results can be explained by the amount of solar radiation received by each façade. The total daily solar radiation is estimated at 2486 Wh/m² and 1514 Wh/m² for the South and the North orientation respectively. The obtained temperatures for the East and West directions are higher due to the long exposure time, and to the important amount of the incident daily radiation, which is of the order
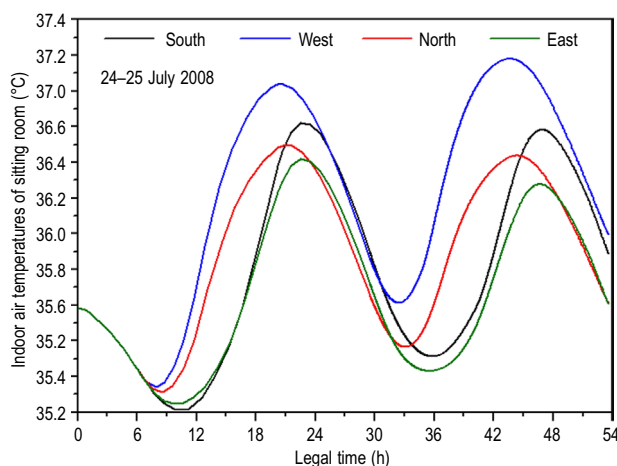

Fig. 7. Sitting room temperatures, S/V ratio = 0.5882, July 24 and 25, 2008
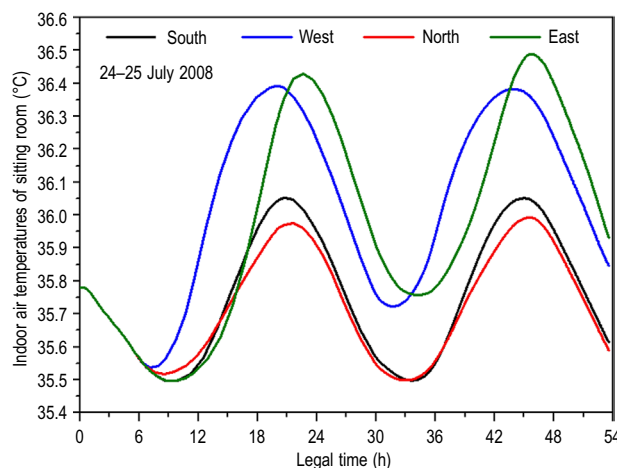

Fig. 8. Sitting room temperatures in the case of stone, S/V ratio = 0.27, July 24 and 25, 2008

of about 4025 Wh/m². We can also draw that internal temperatures of the room are great for west orientation during most of the day (before 20:00), then they become the lower in the morning. These observations coincide with the long duration and timing (morning or evening) of exposure which is always justified by the thermal phase shift caused by the high thermal inertia. We conclude that the building orientation depends largely on the compactness index and the contact mode with the outside.

5.1.2. According to building materials

For the region of Ghardaïa, the influence of orientation changing depends on the floors and exterior walls constructing materials, the insulation levels and application of the inseparable rules of the bioclimatic design (Bekkouche *et al.* 2011, 2013a, 2013b; Cherier *et al.* 2013). For enhanced thermal insulation (the use of

massive brick for example: type-2 wall). Figure 9 confirms almost the same observed scenario for the case of stone described in Figure 7, the difference appears only at the order of values.

However, we spent another study to appear the influence of the orientation of this habitat during the winter, January 06 and 07, 2013. We selected two days characterized by a totally clear sky and an outdoor ambient temperature between 8 and 19 °C, the maximum value is reached around 16:30. The wind speed varies between 0 and 2.5 m/s. Numerical simulation certifies that the positive orientation is the Southern whose compactness index of the construction equal to 0.27 (Fig. 10). One can interpret this result by the fact that the amount of the incident solar radiation on the Southern wall is the highest. By numerical calculation, the daily global radiation incident on the South wall is estimated at 6602 Wh/m^2. The Northern orientation is

less favorable due to the very low amount of the incident solar radiation (251 Wh/m^2) which is much less than the amount of the incident solar radiation on the East and West walls (2373 Wh/m^2).

The calculated values of daily global radiation are based on work previously published (Yaïche, Bekkouche 2008, 2009, 2010).

5.1.3. According to the building size

In this section, we will study the influence of the enlargement of an individual building fully exposed to the sun (at the roof and walls). The plan enlargement corresponds to multiplying each surface "S" by the "Agr" expansion parameter, and consequently we multiply the internal volume by "Agr$\sqrt{Agr}$".

With respecting results of the literature and reference (Bekkouche *et al.* 2013a), the obtained temperatures for each area prove that the enlargement of this construction improves the level of thermal inertia and provide higher thermal insulation performance. The increasing size consolidates the thermal insulation of the building external envelope and allows maintaining and limiting temperature fluctuations. Thermal insulation can keep an enclosed area such as a building warm, or it can keep the inside of a container cold. Therefore, we can discover the appearance of the high thermal inertia which provides more stable temperature change. The calculated temperatures of the internal air in sitting room are given below respectively in Figures 11 and 12 below. The chosen initial conditions are the final conditions of the previous day (23 July).

We consider this time that only the south and north facades are in contact with the outside which corresponds to a compactness index equal to 0.1977, knowing also that the sitting room is subjected to the outside air through one façade that contains the opaque wall and window.

Increasing the size promotes thermal comfort; therefore we must privilege the tall buildings. A very simple example is shown; consider a cube of side length $L = 4$ m, the corresponding index value is 1.25, when we compare to a cube of side length 8 m, we observe that the compactness index of the new cube is 0.625.

In both cases, the most favorable orientation is the North, since firstly, one façade is subject to the external environment and, on the other hand, the obtained values from software designed by Yaïche, Bekkouche (2008, 2009, 2010) show that the received power in the north side is lowermost 1514 (Wh m^{-2}). The
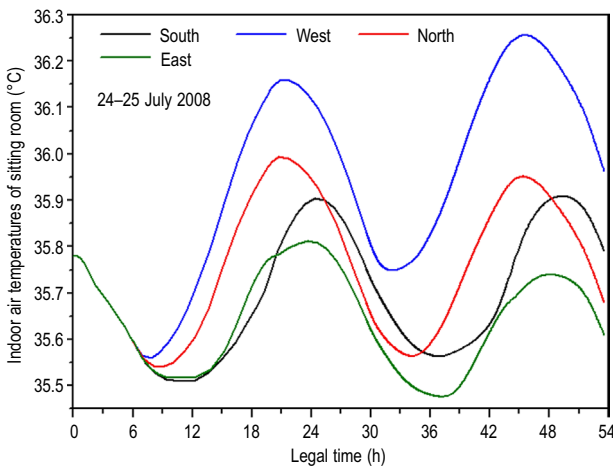

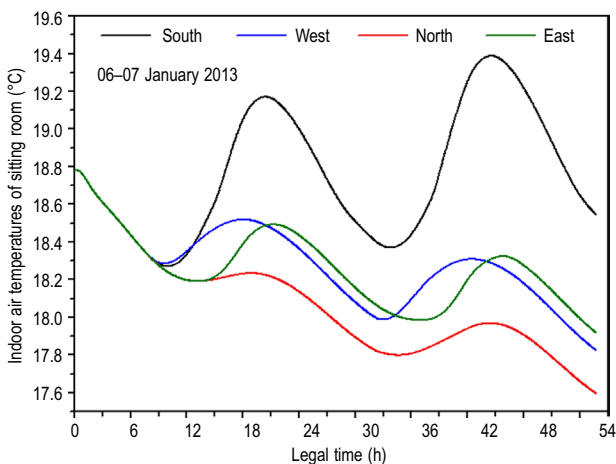Fig. 9. Sitting room temperatures in the case of massive brick S/V ratio = 0.27, July 24 and 25, 2008

Fig. 10. Sitting room temperatures, S/V ratio = 0.27, January 06 and 07, 2013
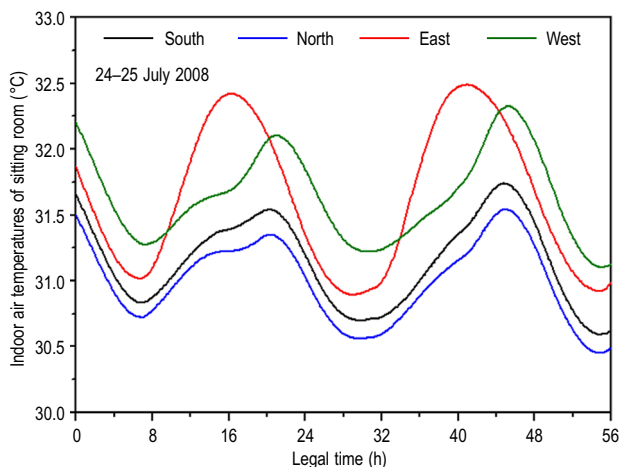
Fig. 11. Sitting room temperatures for an ordinary plane in the case of stone, S/V ratio = 0.1977, July 24 and 25, 2008
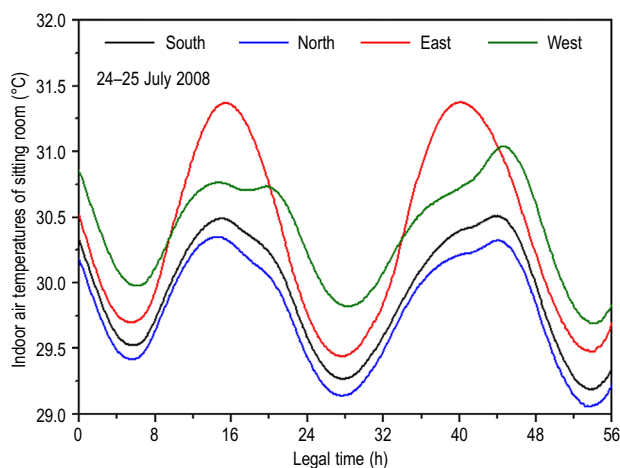

Fig. 12. Sitting room temperatures for an expansion parameter Agr = 3 in the case of stone, S/V ratio = 0.1977, July 24 and 25, 2008

daily solar radiation amounted to 2486 Wh m^{-2} for the vertical South and 4025 Wh m^{-2} for the vertical East and West for the day of July 24. As a result, one can see that the behavior of temperatures undergoes the same scenario by comparing it with the evolution of the incident solar irradiance on different planes.

5.2. Total solar radiation: effect of geometric shapes and heat exchange surfaces

Vertical surfaces are the most critical to the impact of solar radiation. This study examines the effect of geometric shapes on predicting temperature and total solar radiation in the sitting room. Two generic shapes (square and rectangular) have been studied with variations in building orientation using the computer simulation program. Further analysis focuses on the optimum shape for both basic geometric shapes. We show in Table 5 the contribution of the orientation according to geometric shapes. As indicative example, we choose the day of July 25 for the predicted values of the total solar radiation. The obtained values (Yaïche *et al.* 2008, 2009, 2010) show that the daily solar radiation amounted to 2505 Wh m^{-2} for the vertical South and 4022 Wh m^{-2} for the vertical East and West. Table 5 depicts three possible cases:

– Case 1: Total exposure;
– Case 2: Building with two facades, Exposition of South and North walls with exposed roof;
– Case 3: Building with two facades, Exposition of South and North walls with unexposed roof.

From this purely geometric analysis, we propose to compare the change in the zone compactness relative to the geometric shape at constant volume according to the Figure 13. That is to say, by fixing the volume, one can determine the corresponding value of the compactness index. For the sitting room, we choose the following dimensions:

– V = 3.2×10×3 (m^3) for a parallelepipedic form, whose the height is 3 metres.
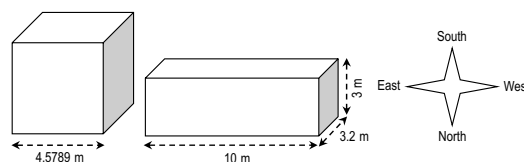– V = 4.5789×4.5789×4.5789 (m^3) for a cubic form.

Fig. 13. Dimensions of the chosen geometric shape

Table 5. Total solar radiation received by the sitting room according to the orientation and geometric shapes

Type of the building exposure	Geometric shape of the sitting room	Compactness index of the sitting room	Total solar radiation received by the sitting room according to the orientation Wh			
			South	East	West	North
Case 1	Parallelepipedic form	0.7458	367110	398052	388270	336540
	Cubic form	0.6552	302830	302830	281470	281470
Case 2	Parallelepipedic form	0.6458	113760	144708	134930	83191
	Cubic form	0.4368	218510	250310	250310	197140
Case 3	Parallelepipedic form	0.3125	75150	120660	120660	44580
	Cubic form	0.2184	52521	84325	84325	31155

For this type of building, the results revealed that the cubic shape with S/V ratio = 0.2184 is the most optimum shape in minimising total solar insolation. The cubic shape of sitting room in a north orientation receives the lowest total solar insolation compared to other orientations.

For the other areas (rooms), this same method is used to determine the appropriate geometrical shape and the optimal orientation of these rooms to derive the optimum orientation of the house.

But for regulating the temperature by controlling solar radiation, we would like to choose the Southern orientation to implement passive bioclimatic design strategies.

Another reason again, the difference between the total solar radiation received by both the Southern and the Northern orientations is not really decisive.

5.3. Time lag and decrement factor

Two factors characterize the wall: the time lag φ and the decrement factor f, defined by Asan and Sancaktar (1998). They were found that thickness of material and the type of the material have a very profound effect on the time lag and decrement factor.

$$\varphi_{min} = t_{Ti,min} - t_{To,min}; \qquad (14)$$

$$\varphi_{max} = t_{Ti,max} - t_{To,max}; \qquad (15)$$

$$f = \frac{T_{i,max} - T_{i,min}}{T_{o,max} - T_{o,min}}, \qquad (16)$$

where $t_{To,min}$, $t_{Ti,min}$, $t_{To,max}$, and $t_{Ti,max}$ are the times when exterior and interior surface temperatures reaches their minima and maxima. $T_{o,min}$, $T_{i,min}$, $T_{o,max}$, and $T_{i,max}$ are the minimum and maximum surface temperatures on the interior and exterior sides.

The time lag " $\varphi = (\varphi_{max} + \varphi_{min})/2$ " is the time required by the maximum (or minimum) of a temperature wave of period P, to propagate through a wall from the outer to the inner surface (Asan, Sancaktar 1998). The decrement factor f is defined as the decreasing ratio of its temperature amplitude during the transient process of a wave penetrating through a solid element. The time lag and decrement factor were extensively studied in the heat transfer literature (Asan, Sancaktar 1998; Asan 2000, 2006; Kontoleon, Eumorfopoulou 2008), as well as their dependence upon wall thickness, materials, thermo physical properties, solar absorptivity...

In our contribution, we are interested in determining the orientation influence on these two factors. The developed simulation model gives Figure 14 which is deduced from the variation of inner and outer surface temperatures of the South wall of sitting room if we refer to Figure 2. The calculated values are given in Table 7, Appendix.

The estimation of the time lag of type-1 wall shows that, because the outdoor and indoor temperatures are not sinusoidal, the values of φ_{max} and φ_{min} are different. An analysis of obtained values shows that the highest time lag (φ = 5 h: 54 min) is that which corresponds to the South orientation while the minimum value is reached by the walls oriented to North. We find by calculation that the time lag for West, North and East directions are 5 h: 17 min, 3 h: 40 min and 4 h: 59 respectively.

Similarly, for the type-2 wall, the South orientation corresponds to the highest value of the time lag. The calculated time lag for South, West, North and East directions are 8 h: 24 min, 7 h: 25 min, 6 h:
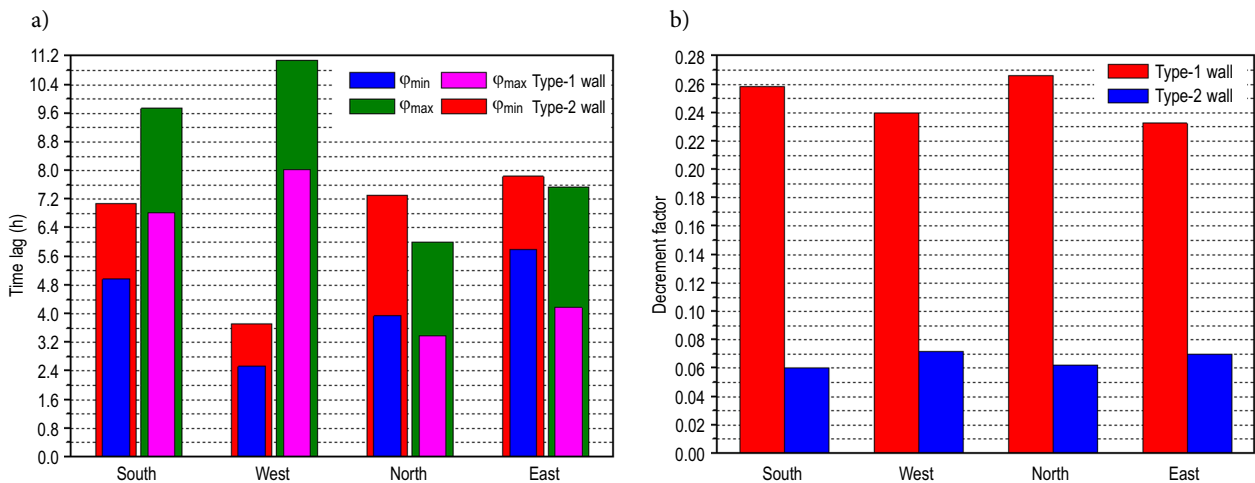

Fig. 14. Time lags φ_{max} and φ_{min} (a) and decrement factor f (b) for type-1 and type-2 walls for a typical summer day, 25 July 2008

40 min and 7 h: 41 respectively. These values are significantly higher compared to the previous case; it is logical, a thermal insulater is a material through which heat moves slowly.

Also walls with low decrement factor are preferred, so from this point of view the type-2 wall is better than type-1. Another consideration must be pointed out. A low decrement factor is not sufficient to ensure the indoor thermal comfort, i.e. a lightweight insulated can have f-values as low as 0.008, but when the initial conditions correspond to very hot temperatures, the indoor air temperature could rise beyond the acceptable comfort limits. The thermal mass of a type-2 wall considerably decreases the exterior temperature swing with an acceptable time delay. Under hot initial temperature, the higher interior air temperature can be caused also by the thermal storage because the brick wall is characterized by both its high thermal inertia, and that better thermal insulation compared to the stone wall.

In conclusion, a sufficient time lag and a low decrement factor will delay the hot outdoor temperature which will comes at the end of the day in the building, period in which it is more easy to cool off with a single opening windows. We can say also that the time lag and the decrement factor depend on the building's orientation.

5.4. Direct solar gain

A direct gain system includes facing windows and a large mass placed within the space to receive the most direct sunlight in cold weather and the least direct sunlight in hot weather. In this type of system, sunlight passes through the windows, and its heat is trapped by the thermal mass in the room. In this situation we will require to change the orientation of the building to determine the direction that reduces the need to use heating and cooling systems by minimizing direct solar gain in summer and maximizing direct solar gain in winter. They are calculated by the following equation:

$$Q_s = 24 \sum I_{sj} S_{sj}, \qquad (17)$$

where Q_s – is the solar gain (Wh), the sum is over all directions j; I_{sj} – is the solar irradiation for orientation j, it is expressed in W/m²; S_{sj} – is the receiving surface of j orientation (m²), is computed as follows:

$$S_{sj} = ASFs, \qquad (18)$$

where A – is the surface openings (m²); Fs – is the correction factor for shading: for Northern $Fs = 0.89$, for

the South $Fs = 0.72$ and finally for the East and West $Fs = 0.67$; S – is the solar factor; is the ratio of the total solar energy flux entering the premises through the glass to the incident solar energy flux., it's all just the contribution of a window to the heating of the room.

Surface openings, South side A = 3.36 m².

Surface openings, North side A = 3.36 m².

Surface openings, East side A = 2.068 m².

Surface openings, West side A = 2.508 m².

Then we deduce S_{sj}: $S_{s\_South} = 1.0644$ m², $S_{s\_North} = 1.3158$ m², $S_{s\_East} = 0.6096$ m² and $S_{s\_West} = 0.7394$ m².

So we can write:

$$Q_s = I_{s\_South}\, S_{s\_South} + I_{s\_North}\, S_{s\_North} + I_{s\_East}\, S_{s\_East} + I_{s\_West}\, S_{s\_West}, \qquad (19)$$

where I_s – is the daily irradiation incident on the considered direction (Wh/m²).

We are required to calculate the average values of daily irradiation calculated for each month and for the four possible orientations in Ghardaïa, El Bayadh and Biskra region (see Table 5).

Table 6 presents values of the average daily solar gain calculated by equation 19 according to the four classical orientations: South, North, East and West. We illustrate also the average daily solar gain of the habitat oriented in full South but with considering that there are not openings in the Northern façade.

Calculations showed that to protect itself from the summer overheating caused by the solar gain, it is recommended to choose the Southern orientation between March and September and the Western orientation for October. On the other hand, to benefit from this solar gain, it is preferably to choose the Eastern orientation for February and Southern orientation between November and January. However, we can say that the prevailing orientation is south. Even if we refer to February and October remarks, we can see that the difference in solar gain is not considerable compared to the Southern orientation. We can also draw from this study that closing openings of North facade reduces the solar gain in hot weather. Consequently, this initial study shows that to effect significant energy savings, special shading systems are needed, combining low solar transmittance in summer with useful solar gain in winter.

Table 6. Average daily irradiation (Wh m⁻²) for Ghardaïa, El Bayadh and Biskra region respectively

	Ghardaïa				El Bayadh				Biskra			
	South and North	East	West	South, No openings in North	South and North	East	West	South, No openings in North	South and North	East	West	South, No openings in North
January	11121	10840	9942	10778	11668	11336	10364	11387	10269	9914	9076	9921
February	11813	11949	11085	11409	12374	12527	11599	12038	11269	11305	10474	10851
March	11438	12147	11447	10935	11733	12523	11789	11313	11194	11771	11076	10664
April	10776	12031	11602	9869	10880	12312	11877	10076	10704	11810	11359	9802
May	s10482	11725	11594	8610	10395	11877	11748	8692	10465	11615	11438	8701
June	10754	11798	11857	8011	10582	11940	11998	8094	10621	11630	11616	8151
July	10344	11419	11393	8040	10221	11581	11557	8125	10290	11296	11214	8157
August	10009	11142	10865	8722	9986	11331	11048	8860	9942	10937	10632	8684
September	10331	11142	10610	9636	10583	11545	10983	10010	10134	10797	10267	9394
October	10802	11070	10351	10273	11289	11605	10824	10863	10325	10483	9795	9764
November	10759	10597	9771	10348	11434	11257	10348	11102	9949	9707	8939	9524
December	10368	9958	9099	10029	10958	10480	9541	10681	9628	9186	8387	9281

Conclusions

The buildings thermal performance can be characterized by the balance between the heat losses and heat gains taking into account their heat storage capacity. In this balance the three fundamental parameters are the insulation level, thermal inertia use and solar radiation control. A new approach to modelling of multizone buildings in Saharan climate was introduced. Thermal nodal method was used to apprehend thermal behavior of air subjected to varied solicitations.

The main findings were summarized as follows:

This simplified method is good approach to the understanding of the thermal behavior of walls and air in a real building. The proposed numerical model is one of the tested methods that correctly predicted the experimental value of the time lag under stable meteorological conditions and a completely clear sky. But, climatic disturbances can cause some problems, especially for estimating the time lag and the decrement factor.

Solar radiation is the most major contributor to heat gain in buildings. In Saharan climate, the highest level of daily average solar insolation is received on the horizontal, followed by the south, east/west and north wall.

Simulated temperatures prove that the optimal building orientation depends largely on the building materials, thermal inertia and compactness index which characterizes the building size, the geometric shape and the contact mode with the outside.

It has be found that to keep the sun of glazed openings in the summer and to let the sun fall on the glass in the winter, south is the most favorable orientation. A building that faces South is generally easier to shade for summer coolness than one that faces East or West. In addition, using southern exposure for solar heat gain is recommended to reduce heating loads in the winter season. Southern exposure allows also using shading strategies to reduce cooling loads caused by direct solar gain on south façades. They have to be equipped with shading devices like overhangs for summer time. These results are coincided with those found by Raychaudhuri *et al.* (1965). From both the experimental observations and the theoretical computations, they found that dwellings facing south-east and south directions have better indoor climatic environment throughout the year. The observed effective temperatures are found to be within the comfort zones only during the winter afternoons while for the rest of the periods of observation in the year; it is beyond the comfort zones in all the houses. On the contrary, in our case, we can not reach the comfort zone for some causes. Wall stone thermal inertia is used for cold storage. It means that walls will accumulate the cold during the night and will restitute it in the air when temperature increases during the day. But in hot arid climates (e.g. desert), the problem is that in summer, outdoor ambient temperatures are almost always high even during the night. Consequently, in very hot period, we can not avoid outdoor heat to come indoor during 24 hours. We can retain that the walls thermal

inertia in these situations, play a contradictory role because the nights are not fresh.

This study guides designers on choosing optimum geometric shape and appropriate orientation for this type of building. The results of parametric analysis indicate that the effect of building shape on total building energy use depends on the building compactness and the level of thermal insulation. With a compact cube shape and with an orientation towards the South-North direction, we can approach to the thermal comfort.

The calculations show that under real meteorological conditions, the time lags and decrement factors of walls change their values depending on the variations of the outdoor temperature, wind velocity, solar radiation and the building's orientation. A sufficient time lag and a low decrement factor will delay the hot outdoor temperature which will comes at the end of the day in the building, period in which it is more easy to cool off with a single opening windows.

The proposed computer program can be coupled with a professional interface that is manipulated by a user-friendly scientists, architects and teachers. The advantage of this program is to integrate the calculated data for optimizing thermal and photovoltaic solar systems.

References

Aksoy, U. T.; Inalli, M. 2006. Impacts of some building passive design parameters on heating demand for a cold region, *Building and Environment* 41(12):1742–1754. http://dx.doi.org/10.1016/j.buildenv.2005.07.011

Anderson, B.; Place, W.; Kammerud, R. 1985. The impact of building orientation on residential heating and cooling, *Energy and Buildings* 8(3): 205–224. http://dx.doi.org/10.1016/0378-7788(85)90005-2

Asan, H.; Sancaktar, Y. S. 1998. Effects of wall's thermophysical properties on time lag and decrement factor, *Energy and Buildings* 28(8): 59–166.

Asan, H. 2000. Investigation of wall's optimum insulation position from maximum time lag and minimum decrement factor point of view, *Energy and Buildings* 32(2): 197–203.

Asan, H. 2006. Numerical computation of time lags and decrement factors for different building materials, *Building and Environment* 41(5): 615–620. http://dx.doi.org/10.1016/j.buildenv.2005.02.020

Auger, J. L.; Alexandre, A.; Martinet, J. 1981. Fonctionnement de Capteurs Solaires Plans en Régime Variable, *Revue Générale de Thermique* 239: 811–824.

Balcomb, J. D.; Hedstrom, J. C.; McFarland, R. D. 1977. Simulation analysis of passive solar heated buildings – Preliminary results, *Solar Energy* 19(3): 277–282. http://dx.doi.org/10.1016/0038-092X(77)90071-8

Bekkouche, S. M. A.; Benouaz, T.; Cheknane, A. 2009. Simulation and experimental studies of an internal thermal insulation of tow pieces of rooms located in Ghardaia (Algeria), *IJACE International Journal of Advanced Computer Engineering* 1(2): 1–6.

Bekkouche, S. M. A.; Benouaz, T.; Cherier, M. K.; Hamdani, M.; Yaiche, M. R.; Benamrane, N. 2013a. Influence of the compactness index to increase the internal temperature of a building in Saharan climate, *Energy and Buildings* 66: 678–687. http://dx.doi.org/10.1016/j.enbuild.2013.07.077

Bekkouche, S. M. A.; Benouaz, T.; Cherier, M. K.; Hamdani, M.; Yaiche, M. R.; Benamrane N. 2013b. Thermal resistances of air in cavity walls and their effect upon the thermal insulation performance, *International Journal of Energy and Environment* 4(3): 459–466.

Bekkouche, S. M. A.; Benouaz, T.; Yaiche, M. R.; Cherier, M. K.; Hamdani, M.; Chellali, F. 2011. Introduction to control of solar gain and internal temperatures by thermal insulation, proper orientation and eaves, *Energy and Buildings* 43: 2414–2421. Elsevier. http://dx.doi.org/10.1016/j.enbuild.2011.05.018

Capderou, M. 1987. *Modeles théoriques et expérimentaux, Atlas solaire de l'Algérie*, Tome 1, Vols 1–2. Office des Publications Universitaires, Algérie.

Cherier, M. K.; Benouaz, T.; Bekkouche, S. M. A.; Hamdani, M.; Benamrane, N. 2013. Improving of interior temperatures by reinforced thermal, insulation of the building envelope in Ghardaïa Climate, *Revue Internationale d'Héliotechnique* 45: 1–7.

Chapman, A. J. 1984. *Heat transfer*. New York: Macmillan.

Chwieduk, D.; Bogdanska, B. 2004. Some recommendations for inclinations and orientations of building elements under solar radiation in Polish conditions, *Renewable Energy* 29: 1569–1581. http://dx.doi.org/10.1016/j.renene.2003.12.018

Cron, F.; Inard, C.; Belarbi, R. 2003. Numerical analysis of hybrid ventilation performance depending on climate characteristics, *International Journal of Ventilation* 1(Special Edition): 41–52.

Dorota, A. C. 2008. Some aspects of modelling the energy balance of a room in regard to the impact of solar energy, *Solar Energy* 82: 870–884. http://dx.doi.org/10.1016/j.solener.2008.04.004

George, S. S. 1999. Architectural utilities 3, *Lighting & Acoustics*. Revised edition, Philippine Copyright. JMC Press. INC. ISBN 971-11-1028-8.

Givoni, B. 1994. Building design principles for hot humid regions, *Renewable Energy* 5(II): 906–916. Elsevier Science.

Givoni, B. 1991. Characteristics, design implications, and applicability of passive solar heating systems for buildings, *Solar Energy* 47(6): 425–435. http://dx.doi.org/10.1016/0038-092X(91)90110-I

Gordon, J. (Ed.) 2001. *Solar energy the state of the art*. ISES position papers, UK.

Haase, M.; Amato, A. 2009. An investigation of the potential for natural ventilation and building orientation to achieve thermal comfort in warm and humid climates, *Solar Energy* 83: 389–399. http://dx.doi.org/10.1016/j.solener.2008.08.015

Hoffman, M. 1983. Solar heating using common building elements as passive systems, *Solar Energy* 30(3): 275–287. http://dx.doi.org/10.1016/0038-092X(83)90157-3

Kasten, F. 1980. A simple parameterization of two pyrhelio-metric formulae for determining the Linke Turbidity factor, *Meteorology Rdsch* 33: 124–127.

Kasten, F. 1996. The Linke turbidity factor based on improved values of the integral Rayleigh optical thickness, *Solar Energy* 56(3): 239–244. http://dx.doi.org/10.1016/0038-092X(95)00114-7

Kasten, F.; Young, A. T. 1989. Revised optical air mass tables and approximation formula, *Applied Optics* 28 (22): 4735–4738. http://dx.doi.org/10.1364/AO.28.004735

Keplinger, D. 1978. Designing new buildings of optimum shape and orientation, *Habitat International* 3(5–6): 577–585. Pergamon press. http://dx.doi.org/10.1016/0197-3975(78)90021-8

Kontoleon, K. J.; Eumorfopoulou, E. A. 2008. The influence of wall orientation and exterior surface solar absorptivity on time lag and decrement factor in the Greek region, *Renewable Energy* 33(7): 1652–1664. http://dx.doi.org/10.1016/j.renene.2007.09.008

Mazioud, A.; Ibos, L.; Dumoulin, J. 2010. Detection of a mosaic hidden behind a plaster layer by IR thermography, in *10th International Conference on Quantitative InfraRed Thermography*, 27–30 July 2010, Québec, Canada.

Mefti, A.; Bouroubi, M. Y.; Khellaf, A. 1999. Analyse critique du modèle de l'atlas solaire de l'Algérie, *Revue des Energies Renouvelables* 2: 69–85.

Howlader M. K.; Rashid, M. H.; Mallick, D.; Haque, T. 2012. Effects of aggregate types on thermal properties of concrete, *ARPN Journal of Engineering and Applied Sciences* 7(7), July 2012.

Mingfang, T. 2002. Solar control for buildings, *Building and Environment* 37: 659–664. http://dx.doi.org/10.1016/S0360-1323(01)00063-4

Mora, L. 2003. *Prédiction des Performances Thermo-aérauliques des Bâtiments par Association de Modèles de Différents Niveaux de Finesse au Sein d'un Environnement Orienté Objet*: Thèse de Doctorat, Laboratoire d'Etude des Phénomènes de Transfert Appliqués au Bâtiment, UFR Sciences Fondamentales et Sciences pour l'Ingénieur, Université de la Rochelle, Septembre 2003.

Morrissey, J.; Moore, T.; Horne, R. E. 2011. Affordable passive solar design in a temperate climate: an experiment in residential building orientation, *Renewable Energy* 36: 568–577. http://dx.doi.org/10.1016/j.renene.2010.08.013

Numan, M. Y.; Almaziad, F. A.; Al-Khaja, W. A. 1999. Architectural and urban design potentials for residential building energy saving in the Gulf region, *Applied Energy* 64(1–4): 401–410. http://dx.doi.org/10.1016/S0306-2619(99)00109-9

Ozel, M.; Pihtili, K. 2007. Optimum location and distribution of insulation layers on building walls with various orientations, *Building and Environment* 42: 3051–3059. http://dx.doi.org/10.1016/j.buildenv.2006.07.025

Pacheco, R.; Ordóñez, J.; Martínez, G. 2012. Energy efficient design of building: a review, *Renewable and Sustainable Energy Reviews* 16: 3559–3573. http://dx.doi.org/10.1016/j.rser.2012.03.045

PN-B-03406:1994. Heating, Calculation of heat load for buildings, volume less than 600 m3 (cancelled). Polish Standard (in Polish).

PN-EN 12831:2006. Heating systems in buildings, Method for calculations of the design heat load. Standard (in Polish).

Raychaudhuri, B. C.; Ali, S.; Garg, D. P. 1965. Indoor climate of residential buildings in hot arid regions, effect of orientation, *Building Science,* 1: 79–88. Pergamon Press. http://dx.doi.org/10.1016/0007-3628(65)90008-3

Rumianowski, P.; Brau, J.; Roux, J. J. 1989. An adapted model for simulation of the interaction between a wall and the building heating system, in *Proceedings of the Thermal Performance of the Exterior Envelopes of Buildings IV Conference*, 1989, Orlando, USA, 224–233.

Sakulpipatsin, P.; Itard, L. C. M.; van der Kooi, H. J.; Boelman, E. C.; Luscuere, P. G. 2010. An exergy application for analysis of buildings and HVAC systems, *Energy and Buildings* 42: 90–99. http://dx.doi.org/10.1016/j.enbuild.2009.07.015

Saulnier, J. B.; Alexandre, A. 1985. La Modélisation Thermique par la Méthode Nodale, Ses Principes, Ses Succès et Ses Limites, *Revue Générale de Thermique* 280: 363–372.

Schmidt, D. 2004. Design of low exergy buildings – method and a pre-design tool, *International Journal of Low Energy and Sustainable Buildings* 3(1): 1–47.

Silvana, F. L.; Celina, F.; Graciela, L. 2009. Thermal behavior of building walls in summer: comparison of available analytical methods and experimental results for a case study, *Building Simulation* 2: 3–18. http://dx.doi.org/10.1007/S12273-009-9103-6

Spanos, I.; Simons, M.; Holmes, K. L. 2005. Cost savings by application of passive solar heating, *Structural Survey* 23(2): 111–130. http://dx.doi.org/10.1108/02630800510593684

TRNSYS16. 2004. *TRNSYS User Annual.* Solar Energy Laboratory, University of Wisconsin Madison, USA.

Yaïche, M. R.; Bekkouche, S. M. A. 2009. Conception et validation d'un logiciel sous Excel pour la modélisation d'une station radiométrique en Algérie, cas d'un ciel totalement clair, *Revue des Energies Renouvelables* 12(4): 677–688.

Yaïche, M. R.; Bekkouche, S. M. A. 2008. Conception et validation d'un programme sous Excel pour l'estimation du rayonnement solaire incident en Algérie, Cas d'un ciel totalement clair, *Revue des Energies Renouvelables* 11(3): 423–436.

Yaïche, M. R.; Bekkouche, S. M. A. 2010. Estimation du rayonnement solaire global en Algérie pour différents types de ciel, *Revue des Energies Renouvelables* 13(4): 683–695.

Appendix

Table 7. Values of time lag, decrement factor and corresponding temperatures for type-1 and type-2 walls, case of a typical summer day, 25 July 2008

	South		West		North		East	
	Type-1 wall	Type-2 wall	Type-1 Wall	Type-2 wall	Type-1 wall	Type-2 wall	Type-1 wall	Type-2 wall
$t_{i,\min}$	10.55	13.17	8.11	9.45	9.52	13.1	11.46	13.98
$T_{i,\min}$	34.53	35.34	35.46	35.71	34.71	35.4	35.31	35.25
$t_{o,\min}$	5.58	6.1	5.58	5.72	5.58	5.79	5.65	6.14
$T_{o,\min}$	30.54	28.89	30.97	28.96	30.53	28.97	31.68	28.91
$\varphi_{\min}$	4.97	7.07	2.53	3.73	3.94	7.31	5.81	7.84
$t_{i,\max}$	21.8	24.94	19.2	22.52	22.31	24.94	22.49	26.03
$T_{i,\max}$	37.55	36.15	39.41	37.09	37.32	36.07	39.88	36.91
$t_{o,\max}$	14.97	15.2	11.16	11.43	18.92	18.93	18.32	18.5
$T_{o,\max}$	42.22	42.29	47.45	48.2	40.34	39.74	51.34	52.69
$\varphi_{\max}$	6.83	9.74	8.04	11.09	3.39	6.01	4.17	7.53
f	0.2586	0.0604	0.2397	0.0717	0.2661	0.0622	0.2325	0.0698

Maamar HAMDANI. Born in Tiaret (Algeria), MSc in physics option: renewable energy from Tlemcen University (2011), researcher in Applied Research Unit on Renewable Energies "URAER Ghardaia", research team: solar and bioclimatic architecture. He has many research papers in international and national journals/conferences. Currently he prepares PhD degree, and he concentrates his studies on developing an adaptive model of thermal comfort in reacting on the orientation, thermal insulation and building materials. He has published many articles in national and International Journals.

Sidi Mohammed El Amine BEKKOUCHE. Born in Nedroma (Tlemcen, Algeria), MSc in Tlemcen University (2006), holds a PhD degree in Physics at Tlemcen University (2009). He was a student of Professor Tayeb BENOUAZ, he works as researcher in Applied Research Unit on Renewable Energies "URAER Ghardaia", research team: solar and bioclimatic architecture. His research field is computational physics, modeling in Physics and simulation of the nonlinear systems, concentrating now on thermal building.

Tayeb BENOUAZ. Born in Ain Sefra (Algeria), MSc in Tlemcen University (Algeria) (1984), PhD in Tlemcen University (1996). His current research interest includes the computational physics, modeling in Physics and simulation of the nonlinear systems, Stability of systems. Director several research projects and has several publications in this field.

Rafik BELARBI. Director of the civil engineering department, LaSIE, University of La Rochelle. His Main responsibilities: Coordinator of the ANR-Habisol project AGROBAT "Agronomy and Building Impact of green roofs on energy perFormance building a multidisciplinary approach". Coordinator of the project ANR-Habisol characterization task: Hygrobat: Towards a method HYGRO-thermal design of efficient buildings. Scientific Head of the European project Marie Curie 7 FP: Exchange of Experience on the Preservation of Historic and Old Water Masonry Structures.

Mohamed Kamel CHERIER. Born in Tiaret (Algeria), MSc in physics option: renewable energy from Tlemcen University (2010), researcher in Applied Research Unit on Renewable Energies "URAER Ghardaia", research team: solar and bioclimatic architecture. He is interested in several areas, such as: thermal standards in buildings, passive and active solar architecture, and adaptive thermal comfort. He has published a number of papers in International Journals and conference proceedings dealing with thermal building.